Contributions to neutron star's tidal deformability from the low density equation of state

A. M. Kalaitzis, T. F. Motta and A. W. Thomas

CSSM and ARC Centre of Excellence for Particle Physics at the Terascale, Department of Physics, University of Adelaide SA 5005 Australia

The low density contribution to the tidal deformability and moment of inertia of a neutron star are calculated via various well known equations of state. The contributions to the moment of inertia are directly calculated, whilst the tidal deformability's are constructed through comparing an equation of state with a fit with the low density region removed. With the recent measurement of GW170817[1,2] providing constraints on the tidal deformability, it is very important to understand what features of the equation of state have the biggest effect on it.

Keywords: Neutron Stars, Tidal Deformability, Low Density, Equation of State, Nuclear Matter, GW170817.

1. Introduction

Neutron stars (NS) being the densest known repositories of nuclear matter contain fascinatingly complex phase changes between their regions of finite and infinite nuclear matter, more commonly known as their layers, denoted crust and core[3–5]. The crust poses challenges with regards to modelling because of the variety of finite nuclei that may appear and complex phase structures that can occur[6].

On the other hand, after the recent GW170817 measurement[1,2], there has been a tremendous push to calculate the tidal deformability (TD) and the moment of inertia (MOI)[7–13] across a variety of equations of state (EOS). This is due to the bounds produced on the TD in Ref 1, 2 of $\Lambda_{1.4} = 190^{+390}_{-120}$, which has recently been analysed via the I-Love-Q relations in Ref. 14 to produce a constraint on the MOI of $\overline{I} = 11.10^{+3.64}_{-2.28}$.

In this paper we explore the proportional contribution that the low density region (LDR) of the EOS makes to the MOI and TD.

2. Theoretical Framework

We will be using the well known EOS shown in Fig. 1 acquired from the online data base in Ref. 15 which details the models in question. In order to calculate the NS profile, ordinarily one would match the model EOS description of the core to some low density EOS in order to account for the NS crust or model it directly[4,6]. We have fit to each EOS using a polytropic of the form given in equation 1 where A, B, C and $D \in \mathbb{R}$. This will act as the EOS without the LDR modelling, with the original EOS data from Ref. 15 containing LDR modelling. As seen in the enlargement in Fig. 1

$$P(\epsilon) = A\epsilon^B + C\epsilon^D. \tag{1}$$

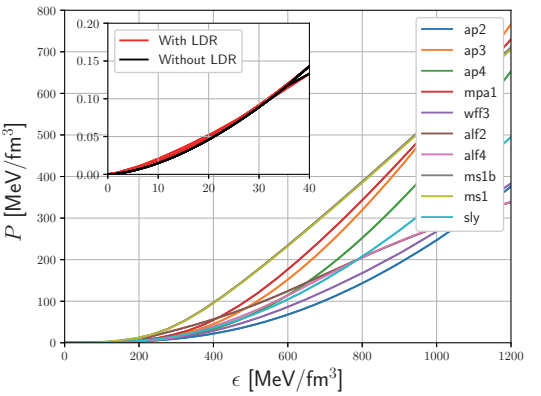

Fig. 1. EOS (pressure P vs energy density ϵ) for all the models[15], nucleon only. Two EOS for each EOS, one with the LDR and one produced from the polytropic fit. The enlargement shows the LDR with all EOS and their fits displayed (There is much overlap between the EOS for the LDR).

We will use these fits to analyse the percentile contributions to the TD via direct comparison of their values. This is done as the TD is defined mathematically as a boundary point and not something cumulative (e.g. integral)[16,17], so that the direct calculation of its LDR contribution is impossible. This is equivalent to modelling a core only NS, consisting of only infinite nuclear matter. The LDR contribution to the MOI may be calculated directly as it is defined as a cumulative integral[18,19].

The NS masses are obtained by numerically integrating the Tolman-Oppenheimer-Volkoff (TOV) equations[20]

$$\frac{\mathrm{d}P}{\mathrm{d}r} = -\frac{(P(r)+\epsilon(r))(m(r)+4\pi r^3 P(r))}{r(r-2m(r))}, \tag{2}$$

$$\frac{\mathrm{d}m}{\mathrm{d}r} = 4\pi r^2 \epsilon(r), \tag{3}$$

until $P(r = R) = 0$ (R the radius of the NS). This produces the mass radius relations given in Fig. 2. We will define the variation of a parameter α as $\Delta\alpha/\alpha$, which is reported as the percentage difference of that parameter when compared to its LDR removed counterpart. This is calculated via (MOI variation $\Delta I/I$ is defined differently as seen in Refs. 12, 21)

$$\frac{\Delta\alpha}{\alpha} = \frac{(\alpha_{\text{with LDR}} - \alpha_{\text{Without LDR}})}{\alpha_{\text{with LDR}}}. \tag{4}$$

Note that this requires one parameter to be fixed. For example the compactness parameter $\beta = M/R$, we would fix the mass and look at the variations in the radius or visa versa. The MOI I is calculated through the formula in Refs. 18, 19, with $\Delta I/I$ defined in Refs. 12, 21.

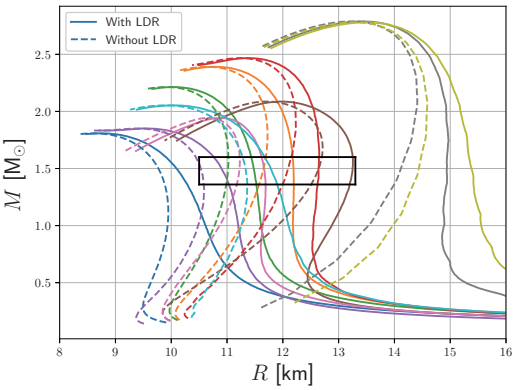

Fig. 2. Mass radius relation for EOS given in Fig. 1. The box represents the 90% confidence constrained mass region given from the GW170817 measurement[1,2]. Mass radius curves retain name and colour convention as in Fig. 1 with dashed versions being the fits.

The tidal Love number, $k_2^{\rm tidal}$, TD, Λ, and binary tidal deformability, $\widetilde{\Lambda}$, equations are verbatim those seen in Refs. 16, 17, 11. For future reference, the TD and binary tidal deformability are calculated via

$$\Lambda = \frac{2}{3} k_2^{\rm tidal} \beta^{-5}, \tag{5}$$

$$\tilde{\Lambda}^{\rm Tid} = \frac{16}{13} \frac{(12q+1)\Lambda_1 + (12+q)q^4\Lambda_2}{(1+q)^5}, \tag{6}$$

where $q = m_2, m_1$ and $m_2 \leq m_1$. With these equations we can now calculate our desired quantities and the percentage contributions from the LDR.

3. Results and Discussion

Numerically solving the MOI equations[11,18,19,21] produces Fig. 3 which shows the proportion of crustal MOI ΔI over the total MOI I. It should be noted that for any realistic star[21] of solar mass

$$0.8 M_\odot \leq M \leq 1.92 M_\odot, \tag{7}$$

we find $|\Delta I/I| < 17.5\%$, with this percentage decreasing rapidly as the mass increases. In particular, a star of solar mass $1.4 M_\odot$ has $|\Delta I/I| < 7.5\%$.

In order to calculate the LDR contribution to the tidal deformability, we simply solve the equations in Refs. 16, 17 for each set of mass radius curves in Fig. 2 and then make use of equation 4 which produces Fig. 4. We find that $|\Delta\Lambda/\Lambda| < 15\%$ for all NS within equation 7's mass range. However, it is important to note that if we disregard the three EOS that lie outside the 90% confidence interval from Refs. 1, 2

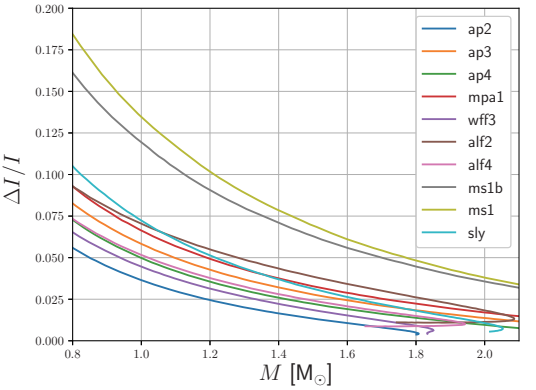

Fig. 3. Percentage of the MOI due to the LDR, scaled via the neutron star's total MOI. Only shown for the EOS with the LDR.

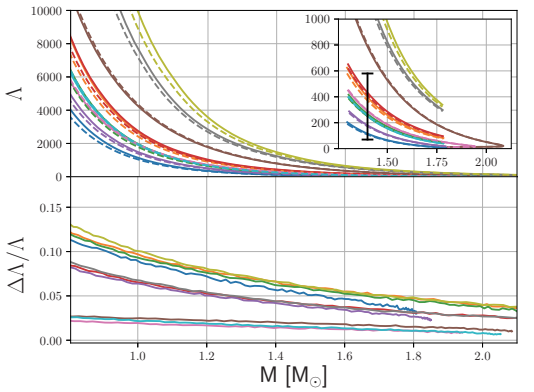

Fig. 4. Percentage of the TD due to the LDR, scaled via the neutron star's total TD. The enlargement shows a shorter range with the black bar representing the bound $\Lambda_{1.4} = 190^{+390}_{-120}$.

in Fig. 4, then our new bounds become

$$|\Delta I/I| < 9.0\%, \qquad |\Delta\Lambda/\Lambda| < 12.0\%, \tag{8}$$

$$|\Delta I/I|_{M=1.4M_\odot} < 3.5\%, \qquad |\Delta\Lambda/\Lambda|_{M=1.4M_\odot} < 7.0\%, \tag{9}$$

within mass range given in Eq. (7). For clarity the tidal Love numbers are displayed in Fig. 5

This happens in spite of the visibly large difference in the mass radius relations (by extension the compactness parameter $\beta = M/R$) and tidal Love numbers shown in Fig. 2 and Fig. 5. The variance in the TD remains relatively low due the large negative power from the β term in Eq. (5).

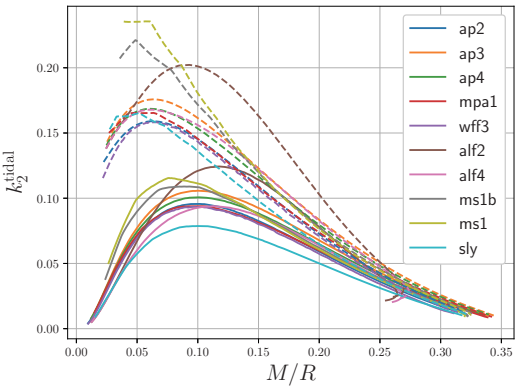

Fig. 5. Tidal Love numbers k_2^{tidal} keeping same conventions as in Fig. 2 and Fig. 1

Due to the low variance in the TD, by extension the variance in the BTD is of a similar order of magnitude as it depends linearly on Λ_1 and Λ_2, with m_1, m_2 being its free parameters, i.e, these two parameters offer no more increase in the variance.

These results have been summarised as the following:

- The impact on macroscopic quantities (e.g. mass, radius etc.) from LDR decreases in significance as the mass increases.
- The TD and MOI are affected to just a small percentage via the inclusion of the low density EOS for all stars with mass $M \geq 0.8M_\odot$, and to a greater extent for stars with mass $M \geq 1.4M_\odot$. Percentages are shown in Eqs. (8) and (9).

This is not to say that the LDR's effects are uniformly negligible, as seen in Fig. 2 where the LDR contributes significantly to the radius. With the imminent measurements of the neutron star radii by NICER, this low density EOS modelling will prove incredibly significant in ascertaining correct predictions for the radius.

4. Conclusion

In summary we see that despite the LDR's proportionally significant contribution to the radius and percentage of the NS content, its contributions to the TD and MOI are small, especially when considered for a star of $1.4M_\odot$ or greater.

Acknowledgements

This work was supported by the University of Adelaide and the Australian Research Council through grants DP150103101 and DP180100497 and the Masters (No Honours) academic scholarship.

References

1. B. P. Abbott *et al.*, Properties of the binary neutron star merger GW170817 (2018).
2. B. P. Abbott *et al.*, GW170817: Measurements of neutron star radii and equation of state, *Phys. Rev. Lett.* **121**, p. 161101 (2018).
3. F. Weber, Strange quark matter and compact stars, *Progress in Particle and Nuclear Physics* **54**, 193 (2005).
4. H. Sotani, K. Iida and K. Oyamatsu, Probing crustal structures from neutron star compactness, *Monthly Notices of the Royal Astronomical Society* **470**, 4397 (06 2017).
5. N. K. Glendenning, *Compact stars Nuclear physics, paricle physicsand general relativity* (Springer, 2000).
6. N. Chamel and P. Haensel, Physics of neutron star crusts, *Living Reviews in Relativity* **11**, p. 10 (Dec 2008).
7. J. B. Wei, A. Figura, G. F. Burgio, H. Chen and H. J. Schulze, Neutron star universal relations with microscopic equations of state (2018).
8. S. De, D. Finstad, J. M. Lattimer, D. A. Brown, E. Berger and C. M. Biwer, Tidal Deformabilities and Radii of Neutron Stars from the Observation of GW170817, *Phys. Rev. Lett.* **121**, p. 091102 (2018).
9. S. Han and A. W. Steiner, Tidal deformability with sharp phase transitions in (binary) neutron stars (2018).
10. Z. Carson, A. W. Steiner and K. Yagi, Constraining nuclear matter parameters with GW170817, *Phys. Rev.* **D99**, p. 043010 (2019).
11. T. Zhao and J. M. Lattimer, Tidal Deformabilities and Neutron Star Mergers, *Phys. Rev.* **D98**, p. 063020 (2018).
12. Z. Qian, R. Y. Xing and B. Y. Sun, Moments of inertia of neutron stars in relativistic mean field theory: the role of the isovector scalar channel (2018).
13. P. Landry and B. Kumar, Constraints on the moment of inertia of PSR j0737-3039a from GW170817, *The Astrophysical Journal* **868**, p. L22 (nov 2018).
14. P. Landry and B. Kumar, Constraints on the moment of inertia of PSR J0737-3039A from GW170817, *Astrophys. J.* **868**, p. L22 (2018).
15. Observations and models of compact stars, EOS available from `http://xtreme.as.arizona.edu/neutronstars/`.
16. S. Postnikov, M. Prakash and J. M. Lattimer, Tidal Love Numbers of Neutron and Self-Bound Quark Stars, *Phys. Rev.* **D82**, p. 024016 (2010).
17. K. S. Thorne and A. Campolattaro, Non-Radial Pulsation of General-Relativistic Stellar Models. I. Analytic Analysis for L $\geq= 2$, *Astrophys. J.* **149**, p. 591 (September 1967).
18. J. B. Hartle, Slowly Rotating Relativistic Stars. I. Equations of Structure, *Astrophys. J.* **150**, p. 1005 (December 1967).
19. J. B. Hartle and K. S. Thorne, Slowly Rotating Relativistic Stars. II. Models for Neutron Stars and Supermassive Stars, *Astrophys. J.* **153**, p. 807 (September 1968).
20. J. R. Oppenheimer and G. M. Volkoff, On massive neutron cores, *Phys. Rev.* **55**, 374 (Feb 1939).
21. J. M. Lattimer and M. Prakash, Neutron Star Observations: Prognosis for Equation of State Constraints, *Phys. Rept.* **442**, 109 (2007).